THERMAL FIELD MEASUREMENT DURING WELDING USING INFRARED THERMOGRAPHY

Adrian FLOREA[1], Ștefan Constantin PETRICEANU*[2], Corneliu RONTESCU[3], Ana Maria BOGATU[4], Dumitru Titi CICIC[5]

The Gas Metal Arc Welding (GMAW) welding process is used to make welded joints using different types of materials, where the temperature of the thermal cycle must be carefully monitored. The paper presents the possibility of monitoring the temperature of the thermal cycle during welding using infrared thermography. The comparative analysis carried out in relation to the measurements made with the help of contact thermocouples, highlighted the fact that the temperature difference between the two methods was between 0 and 20^0C, with a maximum error of 2.75%. From the analysis of the obtained results, it can be seen that the infrared thermography method can be successfully applied in the case of monitoring the temperature of the welding process.

Keywords: infrared thermography, cooling time, welding, phase transformation

1. Introduction

Fusion welding processes are processes that involve phase changes in the used materials. They are used in different industrial applications using base materials having different properties. The quality of the obtained welded joint depends to a large extent on the chemical composition of the materials used, the welding process, the welding technology, but also on the correct choice of welding parameters [1].

The thermal cycle during welding influences the distribution of heat in the components to be welded, but also the phase transformations that take place during the solidification of the molten metal pool. The monitoring of the thermal field in the case of welding processes must be carried out to verify compliance with welding technologies and implicitly with important parameters such as:

[1] PhD student, Faculty of Industrial Engineering and Robotics, University POLITEHNICA of Bucharest, Romania, e-mail: florea.adrian1994@gmail.com
[2] Lecturer, Department of Quality Engineering and Industrial Technologies, University POLITEHNICA of Bucharest, Romania, e-mail: petricon@yahoo.com
[3] Prof., Department of Quality Engineering and Industrial Technologies, University POLITEHNICA of Bucharest, Romania, e-mail: corneliu.rontescu@upb.ro
[4] Lecturer, Department of Quality Engineering and Industrial Technologies, University POLITEHNICA of Bucharest, Romania, e-mail: ana_maria.bogatu@upb.ro
[5] Assoc. prof., Department of Quality Engineering and Industrial Technologies, University POLITEHNICA of Bucharest, Romania, e-mail: dumitru.cicic@upb.ro

preheat temperature (T_p), cooling time (from 800 °C to 500 °C - $t_{8/5}$), cooling rate (c_r), etc.

Cooling time $t_{8/5}$ represent the time taken, during cooling, for a weld run and its heat affected zone to pass through the temperature range from 800°C to 500°C. Preheat temperature represent the minimum temperature the base material needs to be before any welding takes place [2]. The use of inappropriate parameters can cause unwanted structural changes and automatically changes in the characteristic properties of the welded joints [3,4].

To monitor the thermal field on the surface of the components, contact methods (contact thermometers or thermocouples) or non-contact methods (pyrometers or infrared thermography cameras) can be used. Many investigators have used thermographic systems for the measurement of temperature distribution and control of welding. Recently, infrared cameras have been widely used to study the real-time welding process [5–7], which are non-contact measure and give results with high accuracy and precision. The information obtained from the camera gives insight into various forms of weld results such as temperature distribution, geometric shape of the welding joints and possible imperfections. The temperature data recorded from the camera can be used to calculate the cooling times that occur in the range of 800–500^{0}C, which is a material phase transformation that a effects the microstructure and mechanical properties. The effects of cooling rate in a high strength, quenched, and tempered steel on GMAW welding have been studied using four process parameters (welding current, arc voltage, travel speed and preheat temperature). The results found that the heat input plays an important role in the cooling rate, which affects microstructure in the heat-affected zone (HAZ) and weld zone (WZ).

The continuous increase in requirements regarding the operating parameters used in production processes (temperature, operating environment and pressure) has led to the development and use of classes of materials with high mechanical properties (yield strength - R_{eH}, tensile strength - R_m, values of impact energy - KV, etc.). The increase in mechanical properties leads to a decrease in the weldability of materials and the need to develop technologies adapted to new materials.

The work presents the possibility of monitoring the thermal field in the case of fusion welding processes, with the help of an infrared thermography camera. The validation of the results obtained by using the infrared thermography camera was carried out by comparing them with the values obtained after the use of contact thermocouples. The resulting temperature profile allows the $t_{8/5}$ parameter value to be calculated which influences the nature and percentage of the phases formed upon cooling and implicitly the mechanical properties of the thermally affected areas (i.e. tensile strength, microhardness).

To achieve the temperature values distribution obtained with the help of the images taken with the infrared thermography camera, an application was created in Matlab R2017a that is capable of "reading" each image of the recorded video file and analyzing it from the temperature point of view and creating a thermal distribution map. Through this application, researchers can accurately assess temperature values during the welding and cooling process and thus identify possible problem areas, thereby contributing to the improvement of the quality and reliability of the welds.

2. Experimental procedure

To analyze the possibilities of visualizing the thermal field and measuring the temperatures in the welded joint area using the robotic GMAW welding process, 6 butt joint samples were made, using 300 x 150 x 12 mm plates, from S890QL low alloy high-strength steel. The filler material was G 89 4 M21 Mn4Ni2CrMo type wire (according to EN ISO 16834-A), a medium alloy wire electrode for gas metal arc welding of quenched and tempered fine grained structural steel [8]. The chemical composition and properties of the materials used are presented in Table 1 and Table 2 [8,9].

Table 1

Chemical composition of the base and filler materials in wt.%.

Materials	C	Si	Mn	Cr	Ni	Mo	V	N	Nb	Ti	Cu	Zr	S	P
S890QL	0.2	0.8	1.7	1.5	2	0.7	0.12	0.015	0.06	0.05	0.5	0.15	0.01	0.02
G 89 4 M21 Mn4Ni2CrMo	0.1	0.8	1.8	0.35	2.3	0.6	-	-	-	-	-	-	-	-

Table 2

Mechanical properties of the used materials.

Materials	Tensile strength (MPa)	Minimum yield strength (MPa)	Elongation (%)
S890QL	940-1100	≥ 890	11
G 89 4 M21 Mn4Ni2CrMo	940 – 1180	≥ 890	≥15

To achieve the welded joint, the edges of the components were processed in accordance with the specifications presented in Fig. 1.

To keep the parameters of the welding process (welding current - I_s, arc voltage - U_a, welding speed - v_s) at constant values, the welding cell presented in Fig. 2 was used: ArcMate 100iBe Fanuc welding robot (Fanuc Corporation, Oshino, Yamanashi, Japonia) and Fronius TPS 4000 welding power source (Fronius International GMBH, Pettenbach, Austria).

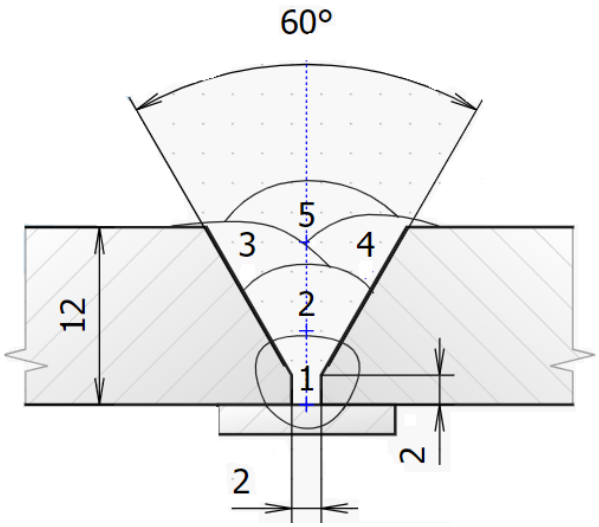

Fig. 1. Sketch of the welded joint
1, 2, 3, 4 and 5 – welding pass

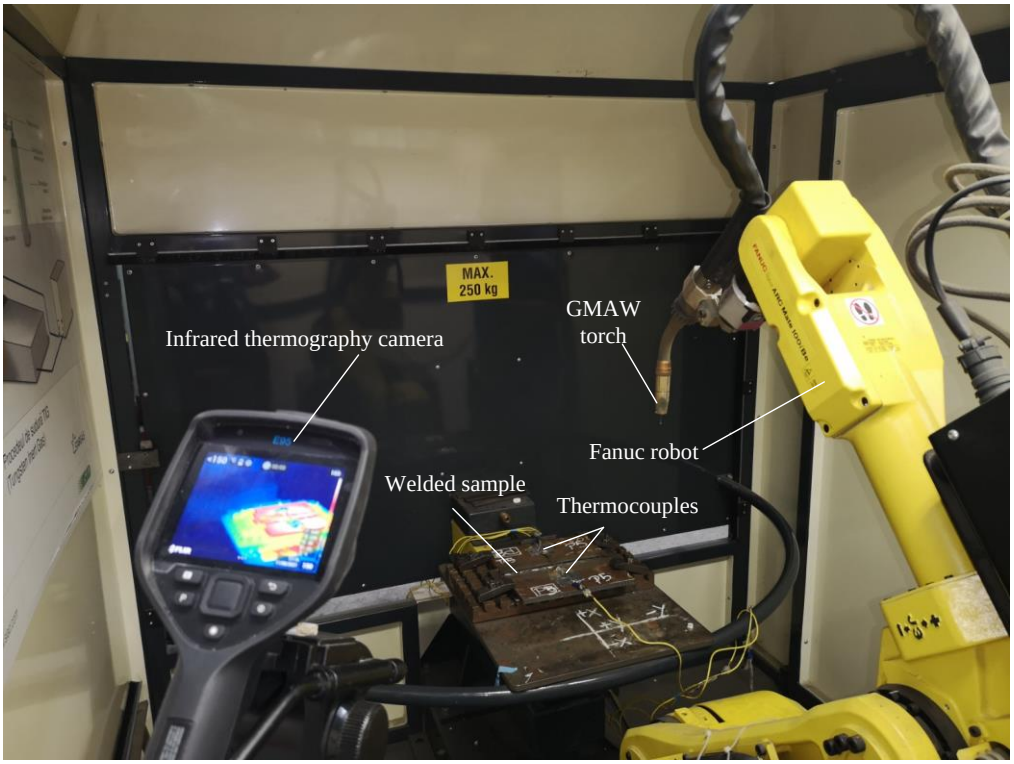

Fig. 2. Fanuc robot cell welding workstation

After the mechanical processing of the joints in accordance with the specifications presented in Fig. 1, the components were fixed in the devices and welded in the robotic cell using the welding parameters in Table 3.

Table 3

The welding parameters used in the experiments

Sample number	Transfer mode	T_{pr} * [^{0}C]	$t_{8/5}$ [s]	Q* [KJ/mm]	I [A]	U [V]	v [mm/s]
1	SPRAY-ARC	100	8	0.84	261	26.9	7
2		150	8	0.72	260	26	8
3		100	12	1.03	290	29.3	7
4		150	12	0.88	270	26.8	7
5		100	17	1.23	293	29.6	6
6		150	17	1.04	314	31.3	8

* T_{pr} – preheating temperature, Q – heat input (calculated with relation 1)

$$Q = k \cdot \frac{I \cdot U}{v} \cdot 10^{-3} \ [kJ/mm] \quad (1)$$

Where:
- k – thermal efficiency [-]; the value of k for GMAW is 0.8 (acc. to EN ISO 1011-1:2009),
- I – welding current [A],
- U – arc voltage [V],
- v – travel speed [mm/s].

To measure the temperature in the welded joint area and establish the temperature distribution on the surface of the welded components (Fig. 3), contact thermocouples were used together with the Graphtec GL 200 temperature recording equipment (Graphtec Corporation, Yokohama, Japan) as well as the infrared thermography camera FLIR E95 (Teledyne FLIR LLC, Wilsonville, Oregon, USA).

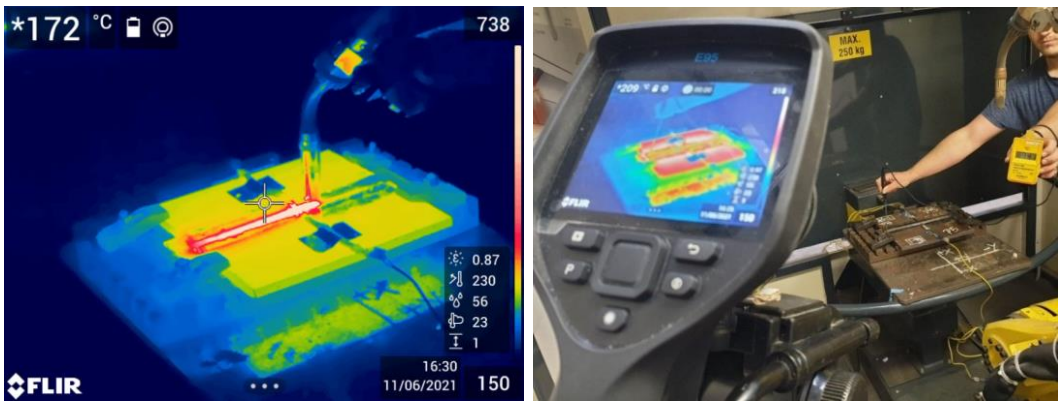

Fig. 3. Stand for temperature measurement using contact thermocouples and infrared thermographic camera

To identify the temperature distribution, it is necessary to know and visualize its value at any point and at any time of the welding process. The FLIR E95 infrared thermography camera offers the possibility of recording in the following conditions:

- optical resolution of 640 × 480 pixels,
- thermal resolution of 40 [mK] at 30 [°C],
- frame rate of 30 [Hz],
- spectral sensitivity between 7.5 and 14 [μm]
- temperature measurement range between -20 and 1500 [0C].

Fine calibration of the camera parameters (relative emissivity, reflected temperature, humidity, outdoor temperature) was performed using a contact thermometer during the preheating process of each sample and a Testo 623 thermohydrometer (Testo, Lenzkirch, Germany).

3. Results

To carry out a comparative analysis, the values of the temperatures measured with the contact thermocouples and the infrared thermography camera were extracted for two samples, P1 and P2, out of 6. Data collection was carried out from the start of the welding process, one second measurement interval between two values.

The spatial correlation of the temperature examination point in the thermographic image was carried out by considering the point closest to the thermocouple, at 1 mm from it, perpendicular to the axis of the weld bead.

The values of the measured temperatures are presented in Table 4, where: P1 and P2 represent the values of the temperatures taken with the contact thermocouples, and P1IT and P2IT represent the values of the temperatures taken with the infrared thermography camera for sample P1 and sample P2 respectively. To have a comparative assessment of the accuracy of the values measured using the two methods, the measurement error was calculated using the calculation formula:

$$\varepsilon_{Pi} = \frac{Pi - PiIT}{Pi} \ [\%] \quad (2)$$

Where:

ε_{Pi} – measurement error, calculated for both methods of temperature determination

Pi – Value of the temperature measured with the contact thermocouples, P1 și P2

PiIT – Value of the temperature measured with the infrared thermography camera, P1IT și P2IT

Table 4

Measured temperatures values

Time [s]	P1IT [^{0}C]	P1 [^{0}C]	Δ_{TP1}* [^{0}C]	ε_{P1} [%]	P2IT [^{0}C]	P2 [^{0}C]	Δ_{TP2}* [^{0}C]	ε_{P2} [%]
0	100.2	100	-0.2	-0.20	150.3	150	-0.3	-0.20
1	110	109.2	-0.8	-0.73	152.1	154.1	2	1.30
2	133.2	135.1	1.9	1.41	157.7	161.7	4	2.47
3	158.5	161.4	2.9	1.80	168.2	172.2	4	2.32
4	209.3	214.1	4.8	2.24	181.5	186.5	5	2.68
5	331	334.3	3.3	0.99	197.5	202.5	5	2.47
6	601.2	600.2	-1	-0.17	209.6	214.6	5	2.33
7	1058	1065	7	0.66	228.2	232.2	4	1.72
8	983.6	981.6	-2	-0.20	274.1	275.5	1.4	0.51
9	884.2	880	-4.2	-0.48	390.9	395.9	5	1.26
10	806	801	-5	-0.62	679.2	685.2	6	0.88
11	739.1	738.4	-0.7	-0.09	998.5	1003.5	5	0.50
12	683	680	-3	-0.44	1001.4	1012.9	11.5	1.14
13	630.2	634.5	4.3	0.68	935.2	950.2	15	1.58
14	577.5	590.9	13.4	2.27	867.5	879.8	12.3	1.40
15	547.3	555.1	7.8	1.41	794.3	802.5	8.2	1.02
16	521	529.6	8.6	1.62	715.5	735.7	20.2	2.75
17	506.4	512	5.6	1.09	669.7	682.7	13	1.90
18	491.3	500	8.7	1.74	631.1	638.1	7	1.10
19	479.2	484.7	5.5	1.13	594.5	601.3	6.8	1.13
20	471.2	474.8	3.6	0.76	561.2	571.2	10	1.75
21	458.4	461.3	2.9	0.63	532.1	542.1	10	1.84
22	452.1	452.1	0	0.00	508.8	520.7	11.9	2.29
23	439.5	443.3	3.8	0.86	499.3	502.5	3.2	0.64
24	428.6	435.1	6.5	1.49	476.3	486.3	10	2.06
25	426	427.6	1.6	0.37	469.6	473.8	4.2	0.89
26	416.1	420.5	4.4	1.05	462.6	462.6	0	0.00
27	410.6	414.4	3.8	0.92	450.4	452.6	2.2	0.49
28	406.9	408.7	1.8	0.44	435.3	443.3	8	1.80
29	404.2	403.3	-0.9	-0.22	428.2	435.2	7	1.61
30	399.1	398.8	-0.3	-0.08	426.3	428.1	1.8	0.42
31	394.8	394.3	-0.5	-0.13	419.5	421.7	2.2	0.52
32	390.1	389.9	-0.2	-0.05	416.2	416.2	0	0.00
33	386.4	386.1	-0.3	-0.08	409.3	411.4	2.1	0.51

Table 4

Measured temperatures values

Time [s]	P1IT [^{0}C]	P1 [^{0}C]	Δ_{TP1}* [^{0}C]	ε_{P1} [%]	P2IT [^{0}C]	P2 [^{0}C]	Δ_{TP2}* [^{0}C]	ε_{P2} [%]
34	382.2	382	-0.2	-0.05	405.1	407.1	2	0.49
35	378.7	378.4	-0.3	-0.08	401.2	403	1.8	0.45
36	374.8	374.2	-0.6	-0.16	396.6	398.8	2.2	0.55
37	370.5	370.3	-0.2	-0.05	392.1	394.8	2.7	0.68
38	364.3	364.1	-0.2	-0.05	389.8	390.8	1	0.26
39	362.4	361.2	-1.2	-0.33	385.5	386.7	1.2	0.31

*red color indicates the maximum values of the measurement errors; green color indicates the minimum values of the measurement errors

* calculated with relation 3

$$\Delta_{TPi} = Pi - PiIT \quad [^0C] \tag{3}$$

Based on the temperature values presented in Table 4, the temperature variation graphs (Fig. 4) measured for samples P1 and P2 were drawn in the case of using thermocouples (P1, P2) and infrared thermography camera (P1IT, P2IT).

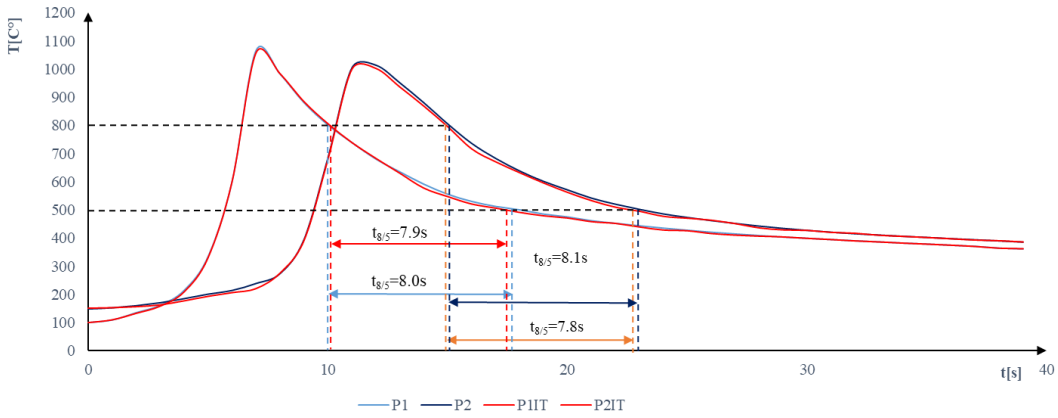

Fig. 4. Variation of thermal cycle temperatures: P1, P2 – temperatures taken using contact thermocouples; P1IT, P2IT – temperatures taken using the infrared thermography camera

Studying the Pearson correlation coefficient between the two sets of experimental data obtained by measuring the post-weld cooling temperature using thermocouples and infrared thermography, helps to understand the concordance and consistency between the two measurement methods.

It provides relevant indications about the validation of the results, the concordance evaluation or the identification of possible significant differences between the two evaluated series.

The formula for calculating the Pearson correlation coefficient is presented in relation 4:

$$r = \frac{\sum_{i=1}^{n}(x_i - \bar{x})(y_i - \bar{y})}{\sqrt{\sum_{i=1}^{n}(x_i - \bar{x})^2}\sqrt{\sum_{i=1}^{n}(y_i - \bar{y})^2}} \quad (4)$$

where:

r - is the Pearson correlation coefficient,

n - is the number of value pairs in the data series,

x_i, y_i - are the individual values in the two data series,

$\bar{x}$, $\bar{y}$ - are the arithmetic means of the x and y data series.

For the first data sets regarding sample 1, P1 and P1IT, the Pearson correlation coefficient is 0.99983 while for the series regarding sample 2 this coefficient has the value 0.99988.

These values, very close to 1, indicate a strong linear relationship between the two measurement methods, suggesting that both methods provide consistent results and can be used interchangeably. Therefore, the two measurement methods can detect temperature variations in a similar way, which helps to confirm the accuracy and reliability of the experimental data.

For a further analysis of the measurement errors, obtained following the application of calculation relation 2, it was proposed to follow their evolution as in Fig. 5.

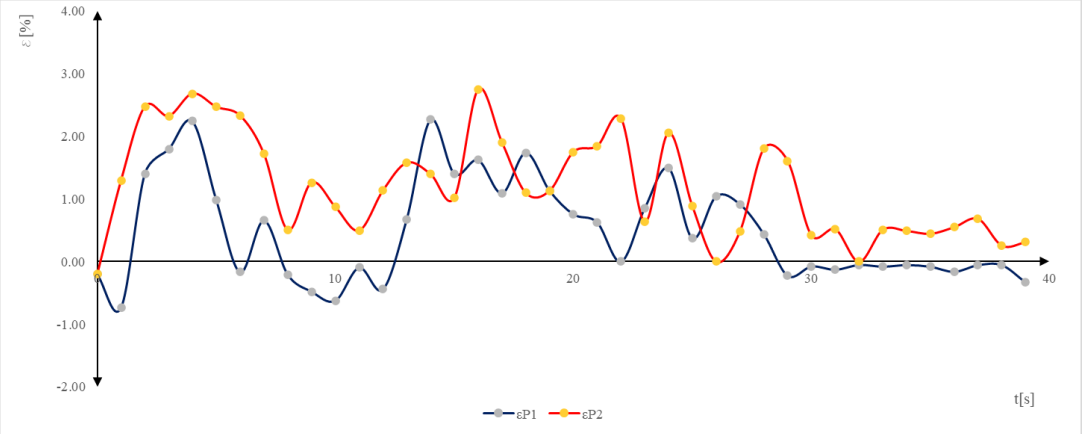

Fig. 5. Variation of measurement errors for the two methods: ε_{P1} – error variation for sample P1, ε_{P2}– error variation for sample P2

Following the analysis of the graphs presented in Fig. 4 and Fig. 5, but also of the temperature values presented in Table 4, one can observe that there are differences regarding the values taken using the two measurement methods. In the

case of sample P1, the maximum difference is 13.4^0C and the maximum error is 2.27%. In the case of sample P2, the maximum difference is 20.2^0C and the maximum error is 2.75%.

The graphs presented in Fig. 4 and Fig. 5 provide information on the variation of the thermal cycle temperatures at a certain point of the samples subjected to the welding process.

From the point of view of thermal cycle variation, it is important to know at every moment, at every point in the image plane, the temperature of the base material and the seam. Its representation in shades of color according to the color palette of the infrared thermography device, does not allow further numerical analysis to observe the thermal profile.

For this reason, a specialized application was created in the Matlab IT solution that is capable of "reading" each image of the recorded video file and analyzing it from the point of view of its temperature and displaying its thermal distribution.

To have an overview of how the temperature evolved in the image plane, the numerically reconstructed 3D graph was plotted in Matlab, by normalizing the temperature values at each important time point for the process (Fig. 6).

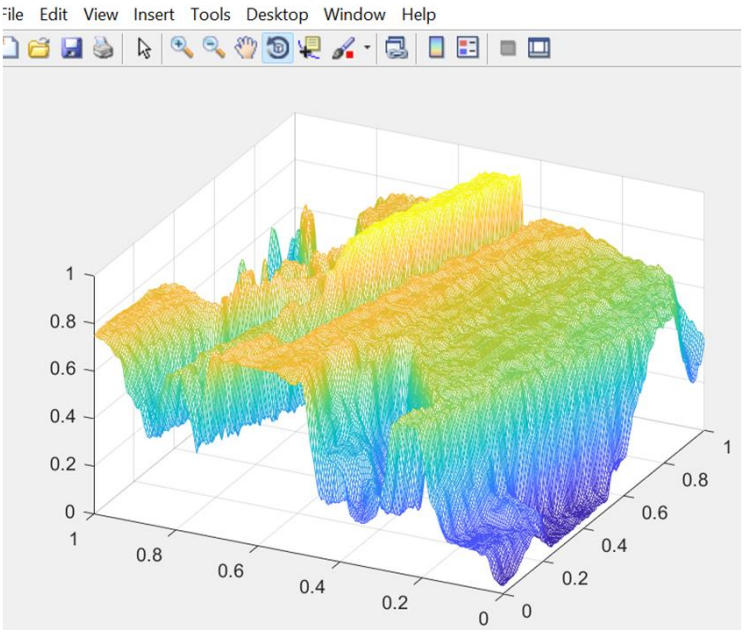

Fig. 6. The 3D profile of the normalized temperature for sample P1, at the particular value of t=36 sec

The image shows a temperature "ridge", with a relatively constant width, along the axis of the welded joint. The relatively constant width of the profile is

given by the shape of the welding source as well as the used welding parameters. The progressive increase in temperature along the seam is explained by the more pronounced temperature dissipation (by conduction to the base material, convection to the air in the environment and radiation to the surrounding objects) in the beginning part of it and keeping it relatively constant (for the analyzed time period) towards the end.

Bilaterally, on the left and right, two areas with apparently lower temperatures can be observed, even more visible as one moves towards the end point of the cord. This phenomenon has no counterpart in the physical reality of the experiment, its presence in the numerical image being explained based on the angle of inclination between the axis of the infrared thermography camera and the vertical plane on the surface of the cord that contains its axis. Additionally, the influence of the angle of exposure to the examined surface is added, respectively of the shape of the joint that places the lateral parts under different incidences than those of the upper part of the sample.

6. Conclusions

The variation of the thermal cycle during welding influences the phase transformations of the materials used and, implicitly, their properties. Considering this aspect, it is important to respect the homologated welding technology and to monitor the temperature of the thermal cycle.

In the paper, the possibility of using infrared thermography as a method of monitoring the thermal field was analyzed in comparison to the classical method in which contact thermocouples were used.

The Pearson correlation coefficient for the data series recorded using the thermocouple and the infrared thermography camera for both sample 1 and sample 2 have values very close to 1, which represents a strong linear relationship between the two methods measurement, meaning that both methods provide consistent results and can be used interchangeably.

Following the analysis of the measured temperatures using the two methods, for P1 and P2, one can observe that in the case of sample P1, the maximum difference is 13.4^0C and the maximum error is 2.27%.and in the case of sample P2, the maximum difference is 20.2^0C and the maximum error is 2.75%.

Also, with the help of the infrared thermography camera and the specialized Matlab image analysis program, the map of the temperature distribution over the entire surface of the welded samples was made, throughout the extent of the experiments.

From the analysis of the data presented in the paper, one can observe that the values measured with the help of the two methods are close, infrared thermography having the advantage that it is easier to use and does not use direct

contact with the components to be welded, method that requires longer preparation time.

The results obtained and presented in the paper lead to the validation of the measurement method using the infrared thermography camera, as a method of monitoring the thermal field during welding.

Acknowledgments

This work has been funded by the European Social Fund from the Sectoral Operational Programme Human Capital 2014-2020, through the Financial Agreement with the title "Training of PhD students and postdoctoral researchers in order to acquire applied research skills - SMART", Contract no. 13530/16.06.2022 - SMIS code: 153734.

R E F E R E N C E S

[1]. *S. Unnikrishnakurup, C. V. Krishnamurthy, K. Balasubramaniam*, Monitoring TIG welding using infrared thermography – simulations and experiments, Przegląd Elektrotechniczny, **92** no. 4, 2016, pp.1-18.

[2]. EN ISO 1011-2:2001 - Welding - Recommendations for welding of metallic materials, Part 2: Arc welding of ferritic steels, accesed in 14.03.2023

[3]. *T.J. Tarn* et al., Robotic Welding, Intelligence and Automation, LNEE, **88**, pp. 369–374, 2011.

[4]. *R. Celin, J. Berneti, D. Anica, S. Balanti*, Welding of the steel grade S890QL, Materials and technology, **48**, 2014, pp. 931–935

[5]. *X.F Liu, C.B. Jia, C.S. Wua, G.K. Zhang; J.Q Gao*, Measurement of the keyhole entrance and topside weld pool geometries in keyhole plasma arc welding with dual CCD cameras, J. Mater. Process. Technol. **248**, 2017, pp.39–48.

[6]. *J.E. Pinto-Lopera, J.M.S.T. Motta, S.C.A. Alfaro*, Real-Time Measurement of Width and Height of Weld Beads in GMAW Processes, Sensors 2016, **16**, pp.1-14.

[7]. *B. Silwal, M. E, Santangelo*, Effect of vibration and hot-wire gas tungsten arc (GTA) on the geometric shape, J. Mater. Process. Technol. 2018, 251, pp. 138–145.

[8]. *G.R. Mohammed, M. Ishak, S.N. Aqida, H.A. Abdulhadi*, Effects of Heat Input on Microstructure, Corrosion and Mechanical Characteristics of Welded Austenitic and Duplex Stainless Steels: A Review, Metals 2017, **7**, 39, pp. 1-18.

[9]. *A. Arora, G.G. Roy, T. DebRoy*, Cooling rate in 800 to 500^0 C range from dimensional analysis. Sci. Technol. Weld. Join. 2010, **15**, pp.423–427.

[10]. *K. Poorhaydari, B.M. Patchett, D.G. Ivey*, Estimation of Cooling Rate in the Welding of Plates with Intermediate Thickness. Weld. J. 2005, **10**, pp.149–155.